

Internal Friction and Microstrain in Polyethylene at 77 K

Norman Brown* and Stephen Rabinowitz

Department of Materials Science and Engineering, University of Pennsylvania, Philadelphia, Pennsylvania 19041

Received July 18, 2003; Revised Manuscript Received October 27, 2003

ABSTRACT: The stress–strain relationship of high-density polyethylene (PE) was measured with a strain sensitivity of 2×10^{-7} at 77 K. The internal friction was determined from hysteresis loops. It was concluded that below a strain of about 10^{-3} all the nonlinear strain came from the crystalline regions by the motion of screw dislocations. Two internal friction processes were discovered which were associated with (100) [001] and (010) [001] slip. The barrier to the motion of the dislocations is pinning by the rigid amorphous material surrounding the lamellar crystals.

Introduction

The purpose of this paper is to understand the nature of the molecular motion that produces internal friction in high-density polyethylene (PE) at 77 K. Measurements of internal friction at 77 K have been made by Kline et al.,¹ Takayanagi,² and Sinnott³ on single-crystal mats and bulk PE using the conventional experimental methods for determining the usual measures of internal friction such as G'' , $\tan \delta$, and $\log \text{dec}$. These investigations show that the γ peak, which is about 50 K above 77 K, increases with the amorphous content. This fact suggests that some if not all of the molecular motion in the amorphous region is frozen at 77 K. However, from the discussion by Ward,⁴ it is still uncertain whether the molecular motion at 77 K comes entirely from the crystalline region or from both the crystalline and amorphous regions. Rabinowitz and Brown⁵ developed a method for measuring non elastic strains, which are responsible for internal friction, at a strain sensitivity of 2×10^{-7} . Brown and Rabinowitz⁶ decomposed the total microstrain in PE at room temperature into its elastic, amorphous, and crystalline components. The amorphous component at room temperature was much greater than the crystalline component; so it was decided to focus on the crystalline component by restricting the amorphous component at 77 K.

The results of this investigation indicate that at the low stress levels, where internal friction is usually measured, the nonlinear strain occurs only in the crystalline region, necessarily by the motion of dislocations.

Experimental Section

In these microstrain experiments the stress–strain curves at various strain rates and temperatures in the vicinity of 77 K were measured. Details of the experimental method have been described by Rabinowitz and Brown.⁵ A strain sensitivity of 2×10^{-7} was achieved with a capacitance extensometer. The dumbbell-shaped specimens had a diameter of 5.7 mm and a gauge length of 50 mm. When inserting a steel specimen, the apparatus can produce a linear stress–strain curve up to a strain of 10^{-4} . Nonlinearity in the stress–strain curves was detected from the hysteresis loops that were produced by loading and unloading the specimen in tension. Because the extensometer was attached to the shoulders of the dumbbell shaped specimen, the absolute strain is known to $\pm 10\%$, but the strain was reproducible within a precision of $\pm 2 \times 10^{-7}$.

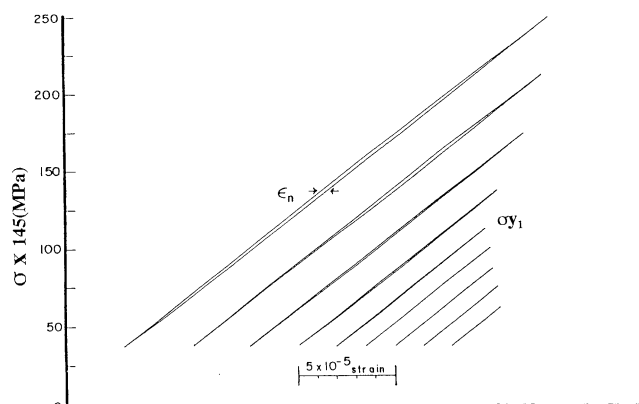


Figure 1. Stress–strain curves of PE at 77 K at various stress amplitudes.

The area of the hysteresis loops was measured with a planimeter. Each loop was measured five times. To avoid erratic behavior in the vicinity of zero stress, it was necessary to maintain alignment by keeping a minimum stress of 0.3 MPa on the specimen. During a load–unload cycle the temperature was constant within ± 0.01 K. The HDPE was injection molded at 463 K in the form of 12.5 diameter rods and after machining was annealed in a vacuum at 403 K for 24 h. $M_n = 11\,500$ and $M_w = 144\,000$. Density = 973 kg/m^3 . Specimens in the annealed condition were irradiated by Co^{60} at room temperature with a dose of 80 Mrad. The PMMA was a commercial rod. The LDPE specimen had a density of 914 kg/m^3 .

Results

Typical stress–strain curves with various stress amplitudes are shown in Figure 1. Hysteresis loops were formed at stresses above 0.75 MPa. The formation of hysteresis indicated that a nonlinear strain occurred. The width of the hysteresis loop was taken as the measure of the nonlinear strain, ϵ_n . A closed hysteresis loop indicates that the nonlinear component of the strain is reversible. The stress at which hysteresis first appeared was very reproducible. In Figure 2, stress is plotted against ϵ_n ; note that there is a threshold stress of 0.75 MPa required to initiate ϵ_n . This threshold stress is called the yield point, σ_{y1} , which is a function of temperature and strain rate as shown in Figure 3. The curves in Figure 3 indicate that the molecular motion associated with σ_{y1} has the characteristics of a ther-

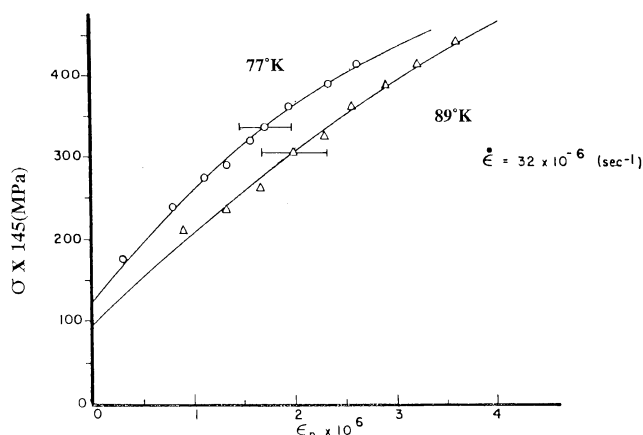


Figure 2. Stress vs the nonlinear strain as measured by the width of the hysteresis loop.

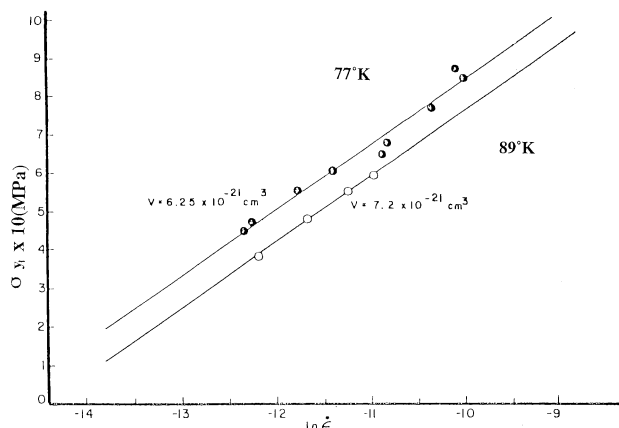


Figure 3. Yield point, σ_{y1} as a function of strain rate.

mally activated process as described by the conventional rate equation,

$$\dot{\epsilon} = A \exp[-(U - \sigma_{y1}v)/kT] \quad (1)$$

where $\dot{\epsilon}$ is strain rate, A is a constant, U is the energy of the barrier, and v is the activation volume. From eq 1

$$v = kT/(\partial\sigma_{y1}/\partial(\ln \dot{\epsilon}))_T \quad (2)$$

$$U - \sigma_{y1}v = H = -Tv(\partial\sigma_{y1}/\partial T)_{\dot{\epsilon}} \quad (3)$$

where H is called the activation enthalpy. From Figure 3 and eqs 2 and 3, $v = 6.25$ and 7.2 nm^3 at 77 and 89 K respectively and $H = 1.9 \text{ kJ/mol}$. The significance of these values will be presented in the discussion.

The energy loss per cycle, ΔW , as determined by the area of a hysteresis loop is plotted against ϵ_n in Figure 4 for different temperatures and strain rates. Each curve has two slopes, which indicates that there are two mechanisms for internal friction. Roberts and Brown⁷ and Brown and Rabinowitz⁶ showed that the change in energy loss with respect to the change in the nonlinear strain may be related to a frictional stress in accordance with the following equation:

$$d\Delta W/d\epsilon_n = 2 \times \text{friction stress} \quad (4)$$

The lower friction stress is called σ_{f1} and the upper one σ_{f2} . The critical stress which initiates the upper internal friction processes is called σ_{y2} . Table 1 shows the

Table 1. Effect of Temperature and Strain Rate on σ_{y1} and σ_{f1}

strain rate (10^{-6} s^{-1})	σ_{y1} (MPa)	$2\sigma_{f1}$ (MPa)
$T = 77 \text{ K}$		
12	0.6	0.51
20	0.68	0.75
32	0.77	0.90
46	0.85	0.95
$T = 89 \text{ K}$		
12	0.53	0.54
23	0.64	0.62
46	0.76	0.82

Table 2. Effect of Temperature and Strain Rate on σ_{y2} and σ_{f2}

strain rate (10^{-6} s^{-1})	σ_{y2} (MPa)	σ_{f2} (MPa)
$T = 77 \text{ K}$		
12	1.73	2.63
20	1.89	
32	2.01	
46	2.14	3.85
$T = 89 \text{ K}$		
12	1.12	2.68
23	1.31	
46	1.57	3.14

dependence of σ_{y1} and $2\sigma_{f1}$ on temperature and strain rate.

The important result is that σ_{y1} is equal to $2\sigma_{f1}$. The following explanation for the lower yield point, σ_{y1} , being equal to twice the friction stress, σ_{f1} , has been given by Brown and Rabinowitz,⁶ who also found this result at room temperature. The explanation will be presented in terms of the motion of dislocations because the results given below indicate that the nonlinear strain occurs in the crystalline region. After the specimen is unloaded, the dislocations are in equilibrium between the friction stress and the restoring stress, "back stress". Upon reloading under tension, the stress used to initiate the motion of the dislocations must equal the friction stress plus the back-stress. If the specimen had been reloaded in compression instead of in tension, the microyield stress would be zero in accordance with the Bauschinger effect.

Figure 5 exhibits the dependence of σ_{y2} on strain rate and temperature. Table 2 contains the effect of temperature and strain rate on σ_{y2} and σ_{f2} .

Note that σ_{f2} is a composite of two internal friction processes; therefore it is expected that σ_{y2} be only approximately equal to two times σ_{f2} . The dependence of σ_{y2} on strain rate and temperature is in accord with eq 1 for a thermally activated process just as for σ_{y1} . The differences in their activation volume and activation enthalpy and their magnitudes will be explained in the discussion in order to understand why there are two yield processes.

To determine the effect of crystallinity, the behavior of the LDPE with a crystallinity of 31% was compared to the behavior of the HDPE with a crystallinity of 81%. In Figure 6 the stress-strain curves of the LDPE and the HDPE are shown. σ_{y1} is the same for both crystallinities. There is however a significant difference in that the more crystalline material exhibits greater nonlinear strain, ϵ_n , for a given stress. This result is important because it indicates that the nonlinear strain, ϵ_n , is produced primarily in the crystals.

To determine whether internal friction might also be contributed by the amorphous region, the behavior of

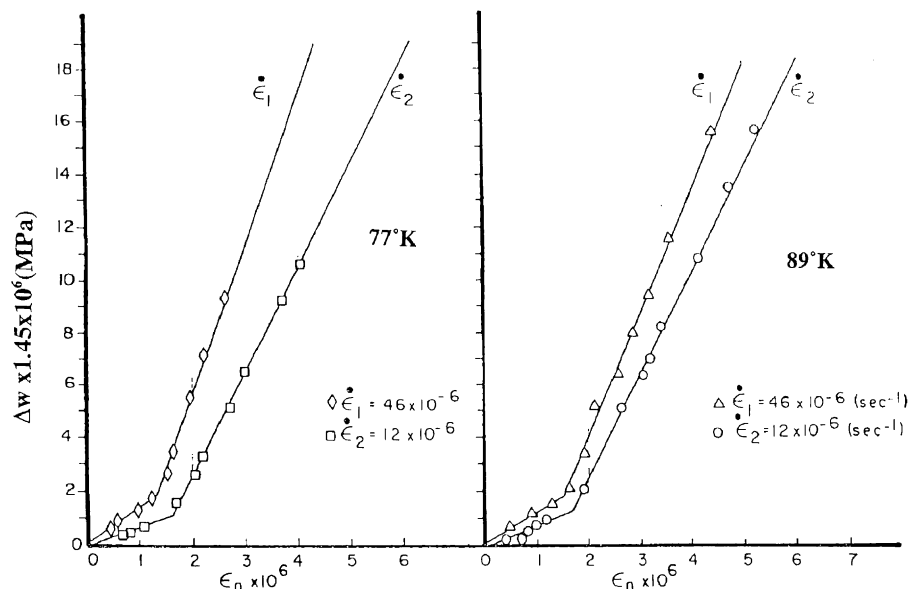


Figure 4. Energy loss per cycle from the area of a hysteresis loop vs the nonlinear strain at different temperatures and strain rates.

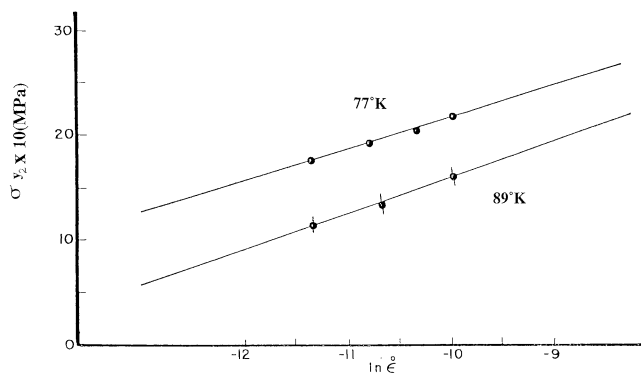


Figure 5. Stress, σ_{y2} , at the break in the energy loss curves in Figure 4, vs strain rate.

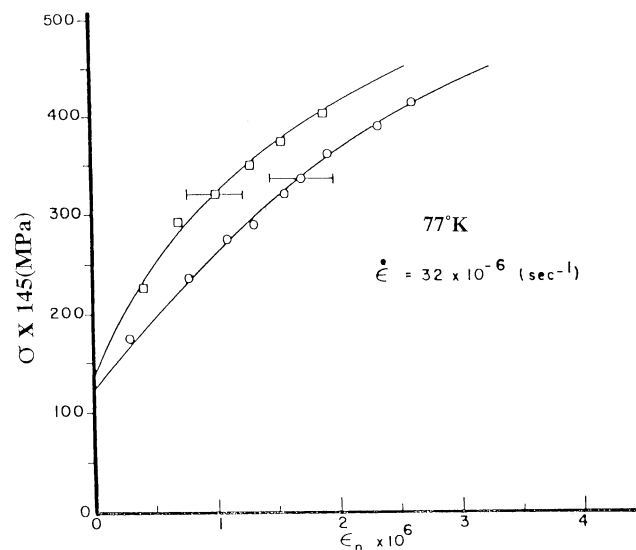


Figure 6. Stress vs the nonlinear strain for (□) low-density and (○) high-density PE.

the completely amorphous polymer, PMMA, was investigated. In Figure 7, the stress-strain curves of PMMA are shown at various stress amplitudes at 77 K. Note that hysteresis is first observed at a stress of 7 MPa,

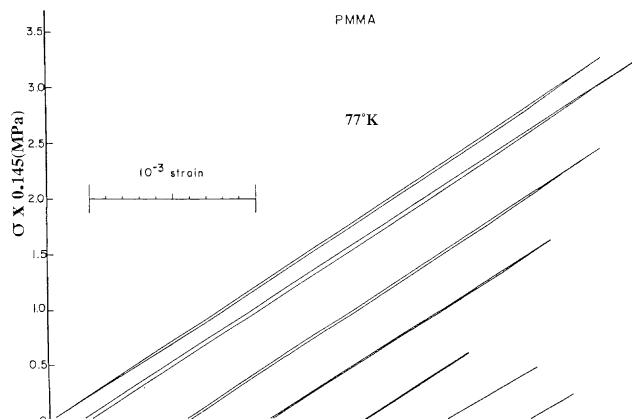


Figure 7. Stress-strain curves of PMMA.

which is about 10 times the stress that initiates hysteresis in PE. This fact suggests that in PE at low stress levels internal friction does not occur in the amorphous region. All the experimental evidence indicates that the internal friction in PE at 77 K occurs in the crystalline region at total strains below about 10^{-3} . Therefore, it follows that the nonlinear strain is best described in terms of the motion of dislocation.

To further understand the influence of morphology on the internal friction, the HDPE was irradiated with 80 Mrad of γ rays from Co^{60} at room temperature. Lu et al.⁸ investigated the effects of dose of γ irradiation in HDPE. They found that the amount of dose had very little effect on the crystallinity and that, for a dose of 80 Mrad, gelation had reached saturation. Many studies of the mechanism of cross-linking in a semicrystalline polymer such as by Chen et al.⁹ on PE indicate that the cross-linking takes place within the amorphous region and also at the boundary of the crystalline region. Figure 8 shows the stress-strain curves at 77 K with various stress amplitudes for the irradiated HDPE. The outstanding feature is that the stress to initiate a hysteresis loop is 16.1 MPa compared to 0.8 MPa for the unirradiated material. It appears that the cross-links in the amorphous region strongly restrict the

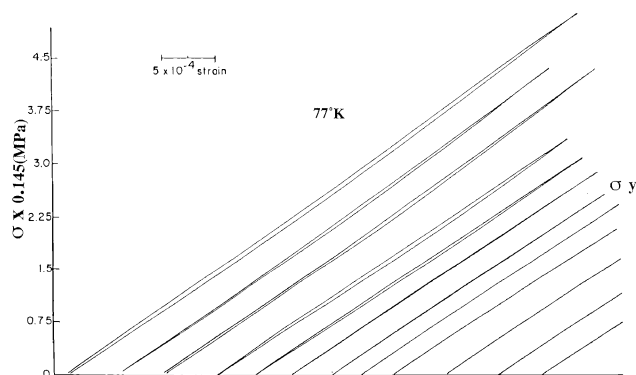


Figure 8. Stress–strain curves for PE irradiated with 80 Mrad of γ rays.

deformation of the crystalline region by hindering the motion of the dislocations.

Discussion

The experimental results lead to the conclusion that the internal friction in PE at 77 K at total strains below about 10^{-3} is produced by deformation in the crystalline region. This conclusion becomes obvious when the basic structure of PE at 77 K is considered. PE consists of very weak crystals which are surrounded by very strong amorphous material, which is well below its glass transition temperature. Weak crystals require a very low stress to move a dislocation in an otherwise perfect lattice where very low stress means that the resolved shear stress is a very small fraction of the shear modulus. This stress is called the Peierls–Nabarro stress. In weak crystals such as zinc and copper, experiments show that a very low stress can move dislocations even at 4 K. A common property of weak metallic crystals is that the inter atomic bonding is isotropic. In the case of PE, the weak isotropic intermolecular van der Waals bonds determine the Peierls–Nabarro stress. On the other hand there is no experimental evidence in the literature that shows that amorphous structures contain easy to move flow units such as dislocations.

The main features of the shear process in PE crystals have been summarized by Bartczak et al.¹⁰ “Fine chain slip (i.e., the translation of individual molecules past each other along the molecular axis) occurs within crystalline lamellae, rotating both the chain axis and the lamellar surface by shear”. The experimental investigations by Bartczak et al.,¹⁰ Bowden and Young¹¹ and Haudin¹² show that the important slip systems are (100) [001] and (010) [001]. In other words slip occurs by screw dislocations lying in the direction of the molecular chains. Lin and Argon¹³ modeled the deformation of quasi–single crystals of Nylon-10 in terms of screw dislocations. Bartczak et al.¹⁰ showed that the critical resolved shear stress for macro yielding at room temperature is 7.2 and 15 MPa on the (100) and (010) plane, respectively. These results suggest that the micro yield stresses σ_{y1} and σ_{y2} may correspond to slip of [001] screw dislocations on the (100) and (010) plane respectively. Since the crystals are randomly oriented, it is expected that both slip systems will be active depending on their orientation with respect to the applied stress, but not active in the same crystal because when the resolved shear stress is maximum in one slip system it is zero in the other. Bartczak et al.¹⁰ showed that PE obeys the Schmid–Coulomb yield criterion where the

Table 3. Activation Volume and Activation Enthalpy for σ_{y1} and σ_{y2}

σ_{y1} (77 K)	$v = 6.25 \text{ nm}^3$	$H = 2340 \text{ J/mol}$
σ_{y1} (90 K)	$v = 7.2 \text{ nm}^3$	$H = 2340 \text{ J/mol}$
σ_{y2} (77 K)	$v = 3.5 \text{ nm}^3$	$H = 8400 \text{ J/mol}$

critical resolved shear stress, τ , is given by

$$\tau = \sigma_y [(\sin 2\lambda)/(2 - k \sin^2 \lambda)] \quad (5)$$

where σ_y is the tensile yield point and λ is the angle between the [001] direction, the chain axis, and the direction of the applied stress. The Coulomb factor, k , was determined by Bartczak et al.¹⁰ to be 0.11 and 0.193 for the (100) [001] and (010) [001] slip systems, respectively. τ is a maximum when $\lambda = 42$ and 39.5° for slip on the (100) and (010) planes, respectively. It follows that internal friction in the microstrain region occurs in those crystals whose chain direction makes an angle with the tensile axis which is in the neighborhood of 40° .

It is of interest to compare the magnitude of the internal friction as measured by ΔW in the present investigation with the internal friction as measured by the conventional methods.

$$\text{specific energy loss} = \Delta W/(\sigma^2/2E) = 2 \tan \delta \quad (6)$$

where E is Young's modulus and has the value of 6.6 GPa. Inserting the values of ΔW from Figure 4 and the corresponding values of σ for the same ϵn from Figure 2 into eq 6 gives values of $\tan \delta = 0.0005$ at the lower strain amplitude and 0.002 at the upper strain amplitude. The latter value is about the same as the average value of $\tan \delta = 0.003$, which is based on the conventional internal friction methods in refs 1–3. The conventional methods of internal friction operated at strain amplitudes above about 10^{-3} whereas we were able to detect the lower energy loss by exploring the range of strains below 10^{-3} .

A more detailed picture of the deformation process is provided by an analysis of the thermal activation mechanism described in eqs 1–3. Table 3 lists the activation volumes and activation enthalpy for σ_{y1} and σ_{y2} .

The activation volume is determined by the equation,

$$v = lab \quad (7)$$

where l is the length of the dislocation, a is the distance the dislocation moves when it overcomes the barrier, and b is the Burgers vector. In our case $b = 0.254 \text{ nm}$ for the [001] screw dislocation. The width of the barrier is not known, but a reasonable assumption is that it is on the order of the intermolecular distance, which from the lattice constants is about 0.6 nm. Along with the values of v in Table 3, l has an average value of about 30 nm. This value is the same as the thickness of the lamella given in the paper by Crist et al.¹⁴ for PE with the same crystallinity of 80%. This means that the length of the screw dislocations that produce the internal friction is equal to the chain length in the lamellar crystals. The next question to be addressed is “How does the motion of the dislocations produce internal friction?”

The cartoon in Figure 9 will help explain the model. The figure represents part of a lamella with the straight lines being the screw dislocations. The surrounding region is the rigid amorphous material. The applied stress, σ , drives the dislocations in a direction that is

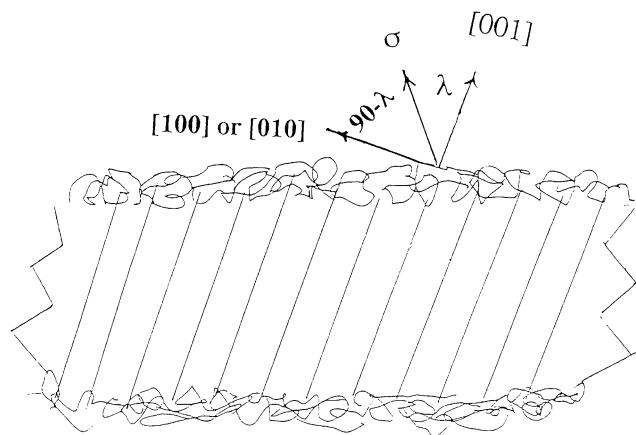


Figure 9. Model for deformation of PE at 77 K showing a portion of a lamella containing screw dislocations parallel to the direction of the molecular chains. The plane of the figure is the (100) or (010), and the surrounding gray area is the rigid amorphous region that pins the dislocations.

perpendicular to their length. Possible obstacles within the crystal are lattice imperfections such as point defects or other dislocations. The model assumes that because the PE was annealed at 130 °C, which is close to the melting point and very slowly cooled, the only imperfections are screw dislocations with the [001] Burgers vector. Edge dislocations and those with other Burgers vectors have a higher energy of formation. Also the Peierls–Nabarro stress is too small to produce lattice friction at the strain rates in this investigation. When a dislocation moves, it produces a displacement at the surface of the crystal. This displacement is obstructed by the amorphous region so that the dislocation is pinned at its ends. A dislocation overcomes this obstacle by the process of thermal activation. Since the strength of the obstacles vary, the dislocations do not move uniformly, and consequently there will be localized pileups of the dislocations. The stress field of the pileups provides the back stress which returns the dislocations to their original position when the specimen is unloaded. The values of the energy of the barrier, $U = H + \sigma v$, are on the order of the energy to break the intermolecular van der Waals bond. U is not expected to be the same for slip on the (100) and (010) planes because the chain folding is different on these planes, and thus, the pinning point should have different strengths. Therein lies the root cause for the two values for the internal friction and for the two microyield points.

The explanation for the fact that a dose of 80 Mrad completely eliminates internal friction at stresses below

16 MPa is straightforward in terms of the model. The ends of the dislocations are strongly pinned by the intensive cross-linking so that it takes a very high stress to move them. It is expected that the stress to produce internal friction would decrease if the dose is decreased especially below the point for complete gelation.

Conclusions

1. Internal friction in PE at 77 K occurs in the crystalline region.
2. Two modes of internal friction were observed: one that was initiated at about 0.8 MPa and the other at about 1.8 MPa. The exact values depends on strain rate and temperature.
3. The internal friction is produced by the slip on the (100) [001] and (010) [001] systems by screw dislocations that extend to the boundaries of the lamellar crystals.
4. The screw dislocations are pinned at their ends by the surrounding amorphous region.
5. The energy loss is produced by the unpinning process as assisted by thermal activation.
6. Internal friction is completely eliminated by 80 Mrad of γ irradiation for stresses below 16 MPa.

Acknowledgment. The work was initially supported by ARPA at LRSM, The Laboratory for Research on the Structure of Matter, and finally completed at LRSM, which is now supported by the NSF.

References and Notes

- (1) Kline, D. E.; Sauer, J. A.; Woodward, A. E. *J. Polym. Sci.* **1956**, 22, 455.
- (2) Takayanagi, M. *Proceedings of the Fourth International Congress of Rheology, Part 1*; Interscience: New York.
- (3) Sinnott, K. M. *J. Appl. Phys.* **1966**, 37, 3385.
- (4) Ward, I. M. *Mechanical Properties of Polymers*, 2nd ed.; John Wiley & Sons: New York, 1983; Chapter 8.4.
- (5) Rabinowitz, S.; Brown, N. *J. Polym. Sci. Part B: Phys.* **2001**, 39, 2420.
- (6) Brown, N.; Rabinowitz, S. *J. Polym. Sci. Part B: Phys.* **2002**, 40, 2693.
- (7) Roberts, J. M.; Brown, N. *Trans AIME* **1960**, 218, 454.
- (8) Lu, X.; Brown, N.; Shaker, M. *J. Polym. Sci., Part B: Phys.* **1998**, 36, 2349.
- (9) Chen, C. J.; Boose, D. C.; Yeh, G. S. Y. *Colloid Polym. Sci.* **1991**, 269, 469.
- (10) Bartczak, Z.; Argon, A. S.; Cohen, R. E. *Macromolecules* **1992**, 25, 5036.
- (11) Bowden, P. B.; Young, R. J. *J. Mater. Sci.* **1974**, 9, 2034.
- (12) Haudin, J. M. *Plastic Deformation of Amorphous and Semi-crystalline Materials*; Escaig, B., G'Sell, C., Ed.; Les Editions de Physique: Paris 1982; p 291.
- (13) Lin, L.; Argon, A. S. *Macromolecules* **1994**, 27, 6903.
- (14) Crist, B.; Fisher, C. J.; Howard, P. R. *Macromolecules* **1989**, 22, 1709.

MA030390K